Vol. 86: 69–84, 2021
https://doi.org/10.3354/ame01959

AQUATIC MICROBIAL ECOLOGY
Aquat Microb Ecol

Published online April 8

Insights into the planktonic to sessile transition in a marine biofilm-forming *Pseudoalteromonas* isolate using comparative proteomic analysis

Zhiwen Wu[1,2,#], Yuyuan Wu[1,2,#], Yanqiu Huang[1], Jian He[1,2], Pei Su[1], Danqing Feng[1,*]

[1]State-Province Joint Engineering Laboratory of Marine Bioproducts and Technology, College of Ocean and Earth Sciences, Xiamen University, Xiamen 361102, PR China

[2]State Key Laboratory of Marine Environmental Science, Xiamen University, Xiamen 361102, PR China

ABSTRACT: Bacterial biofilms play an important role in marine biofouling. The formation of a biofilm starts when marine bacterial cells transition from a planktonic to an attached state. However, the molecular mechanisms involved in this transition are poorly understood. Here, 51 strains of marine bacteria were isolated from natural biofilms growing on submerged artificial surfaces (glass slides, epoxy panels, and bridge pillars) and evaluated for their biofilm-forming capacity. Eleven strains formed relatively strong biofilms and 16S rRNA gene sequence analysis indicated that they belonged to the genera *Leisingera*, *Roseobacter*, *Pseudoalteromonas*, *Alteromonas*, *Tenacibaculum*, *Vibrio*, *Chryseobacterium*, *Aquimarina*, and *Acinetobacter*. Strain *Pseudoalteromonas* sp. W-7 showed efficient and rapid attachment and was therefore chosen for further study. An iTRAQ-based comparative proteomic analysis of planktonic and attached strain W-7 cells was carried out. A total of 3468 proteins were identified, of which 163 showed significant differential expression (120 down-regulated and 43 up-regulated in attached cells relative to planktonic cells). KEGG (Kyoto encyclopedia of genes and genomes) analysis indicated that pyruvate metabolism, carbon fixation, and carbon metabolism were significantly affected in attached cells. Up-regulated proteins such as UTP-glucose-1-phosphate uridylyltransferase, acetyltransferase component of pyruvate dehydrogenase complex, OmpA-like protein, and acetyl-coenzyme A synthetase may be important during initial adhesion. Our findings provide a deeper understanding of the planktonic to sessile transition of marine fouling bacteria.

KEY WORDS: Marine bacteria · *Pseudoalteromonas* · Attachment · iTRAQ · Differentially expressed protein · Biofouling

1. INTRODUCTION

Marine biofouling on the surfaces of submerged artificial structures like vessels, pipelines, bridges, and aquaculture facilities can cause significant economic losses (Yebra et al. 2004, Abioye et al. 2019, Xie et al. 2019). Marine bacteria are usually regarded as early fouling organisms, as they can adhere to and form biofilms on submerged surfaces (Callow & Callow 2002, Abioye et al. 2019, Xie et al. 2019). Marine biofilms themselves can cause serious problems, for example by increasing the drag force on ship hulls, thereby increasing fuel costs and accelerating corrosion (Xu et al. 2017, Hunsucker et al. 2018). Furthermore, marine biofilms can induce the attachment of macrofoulers such as barnacles, tubeworms, and mussels (Bacchetti De Gregoris et al. 2012, Yang et al. 2013, Li et al. 2014, Shikuma et al. 2014, Liang et al. 2019). Thus, investigations into bacterial attachment and biofilm development by bacteria are impor-

#These authors contributed equally to this work
*Corresponding author: dqfeng@xmu.edu.cn

tant in developing a more complete understanding of marine biofouling.

The life cycle of a biofilm can be described in 3 stages: (1) the attachment of planktonic cells to a surface, (2) the growth and formation of 3-dimensional structures, and (3) the detachment and sloughing of the biofilm from the surface (Costerton et al. 1987, Dobretsov 2010). The initial attachment of planktonic cells is a critical stage for biofilm formation, during which bacteria transform from a planktonic to a sessile or adherent lifestyle (Belas 2013, 2014). The biofilm development of marine bacteria has been studied at the molecular level by omics techniques such as proteomics (Ritter et al. 2012, Chandramouli et al. 2013, Leary et al. 2014, Favre et al. 2018). For example, Ritter et al. (2012) performed proteomic comparisons of planktonic cells and biofilms of the marine bacterium *Pseudoalteromonas* sp. D41 and found that 4 outer-membrane proteins were strongly induced in biofilms. Proteomic analysis of biofilm and planktonic phenotypes of the marine bacterium *P. lipolytica* TC8 showed that peptidases, oxidases, transcription factors, membrane proteins, and enzymes involved in histidine biosynthesis were overexpressed in biofilms (Favre et al. 2018).

These studies investigated biofilms formed by marine bacteria after their attachment and proliferation, rather than during the planktonic to sessile transition. Proteins, polysaccharides, and other polymers such as extracellular DNA within the biofilms are produced by the progeny of the initially adhered cells, which may have different metabolic activity than the first generation of cells transitioning from the planktonic state. To specifically investigate the molecular mechanism of the transition process in marine fouling bacteria, it is important to focus on understanding the properties of cells that have adhered to a surface but not yet replicated.

Few studies have addressed the mechanisms underlying the transition from planktonic to attached state in marine fouling bacteria, although there are many studies on the attachment mechanisms of medically important bacteria. Diverse adhesins (such as invasin, YadA, and Ail) and the sensory transduction mechanism termed surface sensing (which often involves rotating bacterial flagella) have been suggested to be involved in the attachment of pathogenic bacteria (Leo & Skurnik 2011, Belas 2014). Furthermore, for bacteria related to infections from implanted medical devices, such as *Staphylococcus epidermidis*, several specific factors are involved in the primary attachment of bacteria to polymer surfaces, including autolysin AtlE, staphylococcal surface protein (Ssp1), and fibrinogen-binding protein (Fbe) (Mack 1999). In marine bacteria, Hoke et al. (2011) explored the membrane proteome of *Pseudoalteromonas tunicata* (commonly found on the surfaces of marine invertebrates and seaweeds) during the transition from planktonic to adherent state using 2-dimensional blue native/SDS PAGE analysis and identified a proteomic change associated with adhesion. However, as with many studies on the attachment mechanisms of pathogenic bacteria, in Hoke et al. (2011) it was unknown whether adherent cells had previously divided.

The aim of this study was therefore to better understand the mechanisms underlying the planktonic to sessile transition in marine bacteria that foul artificial structures. We isolated marine bacteria from natural biofilms growing on submerged artificial surfaces and evaluated their biofilm-forming capacity. Six of the bacterial strains that showed relatively strong biofilm-forming capacity were further tested for their attachment capacity. Strain W-7, a *Pseudoalteromonas* isolate, had a relatively high biomass of attached cells after 3 h of culture of the initial bacterial suspension and was therefore chosen to further explore the attachment mechanism using iTRAQ (isobaric tags for relative and absolute quantification)-based comparative proteomic analysis. An assay to obtain cells of strain W-7 that had attached to a surface but not yet undergone cell division was performed to determine the optimum time to take samples for proteomic analysis.

2. MATERIALS AND METHODS

2.1. Isolation and identification of marine bacteria associated with surfaces

Bacteria were isolated from natural marine biofilms on the submerged artificial surfaces of epoxy panels, glass slides, and concrete bridge pillars. Epoxy panels were submerged for 7 d at a depth of 30 cm in seawater near Dalipuyu Islet (24° 56′ N, 118° 16′ E) in Xiamen Bay, China, in May 2015. Glass slides were submerged for 7 d at a depth of 30 cm in seawater near Dongshan Island (23° 60′ N, 117° 34′ E), Fujian province, China in October 2016. The concrete pillars of Yanwu Bridge (24° 43′ N, 118° 09′ E), Xiamen Island, which are exposed to air during low tide, were chosen for bacterial isolation in May 2016. Each of these surfaces was washed with sterile filtered seawater (FSW, natural seawater filtered through a 0.22 µm filter membrane then sterilized at 115°C for

30 min) to remove sediment and loosely attached bacteria, and then sampled using a sterile cotton swab. Swabs were put into sterile tubes in an icebox and transported to the laboratory. Sterile seawater (5 ml) was added, and tubes were vortexed prior to isolation of strains by serial dilution in sterile seawater and plating on marine agar 2216E plates (Wang et al. 2010). After incubating the plates at 28°C for 48 h, bacterial colonies with different morphologies were isolated and purified.

Identification of isolated bacteria to the genus level was based on 16S rRNA gene sequence analysis. Chromosomal DNA was extracted from bacteria using a TIANamp bacteria DNA kit (TIANGEN Biotech) following the manufacturer's instructions. The 16S rRNA gene sequence was amplified by PCR using primers 27F (5′-AGA GTT TGA TCC TGG CTC AG-3′) and 1492R (5′-GGY TAC CTT GTT ACG ACT T-3′) (Lane 1991). The PCR program consisted of an initial denaturing step at 95°C for 5 min, followed by 30 cycles of denaturation at 94°C for 45 s, annealing at 55°C for 45 s, and elongation at 72°C for 90 s, and a final extension step at 72°C for 10 min. The PCR products were sent to Porui Biotech (Xiamen, China) for sequencing. The 16S rRNA gene sequences were analyzed using the BLAST program from the GenBank database on the National Center for Biotechnology Information (NCBI) website (https://www.ncbi.nlm.nih.gov/).

2.2. Evaluation of biofilm-forming capacity

Biofilm formation was quantified using a modification of the method in Peeters et al. (2008). Each bacterial strain was cultured overnight in 2216E broth on a rotary shaker (150 rpm) at 28°C. Bacterial culture (2 µl) and 100 µl of 2216E broth were added into each well of a 96-well microplate. There were 3 replicate wells for each strain. Control wells contained 102 µl 2216E broth. The 96-well microplates were then incubated at 28°C for 24 h. After 24 h of biofilm formation, the supernatant was removed from each well. To fix the biofilms, 4% formaldehyde was added to each well. After 5 min, the formaldehyde was removed, the plates were rinsed with distilled water, and 200 µl of 0.1% crystal violet was added to each well. After staining for 5 min, excess crystal violet was removed, and the plates were washed with running tap water. The plates were then air dried, and 200 µl of ethanol was added to each well to solubilize bound crystal violet. The absorbance was measured at 600 nm using a microplate reader.

2.3. Evaluation of attachment capacity

Six bacterial strains (W-7, D-1, D-2, D-6, Y-5, and Y-19) were selected for the bacterial attachment assay because they showed relatively strong biofilm-forming capacity, with a crystal violet absorbance of OD_{600} > 0.8. Five other strains (W-8, Y-15, W-2, Y-9, and W-1) also had an OD_{600} > 0.8 but formed flocs during growth, making it difficult to quantify density. The 6 strains selected for further study did not form flocs. The bacterial attachment assay was adapted from Leroy et al. (2007) and Wang et al. (2017). Each strain was grown overnight in 30 ml 2216E broth on a rotary shaker (150 rpm) at 28°C. After centrifugation at a relative centrifugal force of 2760 × *g* for 5 min, the supernatant was removed, and the cells were suspended in sterile FSW at a density of 10^7 cells ml^{-1}. A glass coverslip (24 × 24 mm) was placed into each well of a 6-well plate, and then 5 ml bacterial suspension was added. There were 3 replicates for each strain. The plates were incubated for 3 h at 28°C. Attached bacteria were fixed for 10 min by adding 200 µl of 4% formaldehyde to each well. Then coverslips were washed gently with sterile FSW to remove non-attached bacteria. Attached bacteria on coverslips were stained with 0.1% crystal violet for 10 min. The coverslips were subsequently washed with distilled water and observed under a Leica DMIL inverted microscope at 400× magnification. The number of attached bacteria were counted in 10 random fields of view on each coverslip from photographs taken with a Leica MC170 HD camera.

2.4. Assay to obtain adhered but not yet proliferated bacterial cells

Strain W-7 showed relatively strong biofilm-forming capacity and attachment capacity and was therefore selected for further study. To obtain cells that had settled on the surface but not yet begun to proliferate, the following method was used. Strain W-7 was grown overnight in 2216E broth, and 5 ml of a cell suspension (10^7 cells ml^{-1}) prepared in FSW was added to a coverslip and placed into a 6-well plate. Fifteen coverslips were used, and plates were incubated at 28°C. After 1 h, attached bacteria on 3 replicate coverslips were fixed and stained as described above. The other 12 coverslips were washed gently with sterile FSW to remove non-attached bacteria and added into the 6-well plates, with 1 coverslip per well, each of which contained 5 ml sterile FSW. The

attached bacteria on these 12 coverslips were cultured further at 28°C. At 2 h intervals, bacteria on 3 replicate coverslips were fixed and stained as described above. Thus, bacterial cells that had been cultured for 2, 4, 6, and 8 h beyond the initial 1 h of culture were obtained. Bacterial cells on coverslips were observed and counted as described above. If the average number of bacteria on coverslips at a particular culture time was significantly higher than the number present in the 1 h treatment, it was assumed that the bacteria had proliferated by that time.

2.5. Protein extraction of planktonic and attached cells of strain W-7

Thin circular glass plates (13 cm diameter, 2 mm thick) were used. Before use, the plates were subjected to ultrasonic cleaning in ethanol and were sterilized at 121°C for 20 min. There were 3 replicates of protein samples for the proteomic analysis. Each replicate included 10 glass discs, with each glass disc placed in a separate petri dish containing 70 ml of bacterial cell suspension in FSW with a density of 10^8 cells ml^{-1}. Discs were incubated at 28°C for 3 h. Proteins were extracted from bacterial cells following Mosier et al. (2015). To obtain planktonic cells for each replicate, 30 ml of bacterial suspension was collected by randomly selecting 3 dishes from the replicate and sampling 10 ml of bacterial suspension from each dish. The 30 ml of bacterial suspension was transferred to a tube and centrifuged at 6730 × *g* for 2 min. The pellet was resuspended in 1 ml SDS cell lysis buffer (5% SDS; 50 mM Tris-HCl, pH 8; 150 mM NaCl; 0.1 mM EDTA; 1 mM $MgCl_2$) (Mosier et al. 2015), vortexed for 2 min, and then used for protein extraction. To obtain attached bacterial cells, the glass discs were first washed with sterile FSW to remove non-attached bacteria, and then attached bacteria were removed by repeatedly pipetting 4 ml SDS cell lysis buffer over the bacteria using a 1000 µl pipette until the entire surface of the disc had been washed. This was carried out on 10 glass discs for each replicate to provide sufficient protein (≥100 µg) for proteomic analysis. The SDS cell lysis buffer containing planktonic or attached cell material was heated at 100°C for 15 min, vortexed for 3 min, and centrifuged at 11 060 × *g* for 10 min. The supernatant was mixed with 300 µl of 100% trichloroacetic acid. After overnight precipitation of proteins, the mixture was centrifuged at 21 690 × *g* for 20 min at 4°C. The pellet was washed 3 times with 1 ml cold acetone and air dried. Protein content was determined using a 2-D quant kit (GE Healthcare).

2.6. Protein digestion and iTRAQ labeling

For each replicate of attached and planktonic cells, a protein sample (100 µg) was added to a tube and mixed with urea lysis buffer (7 M urea; 4% SDS) to a volume of 100 µl, and 10 mM tris(2-carboxyethyl)-phosphine (Thermo Fisher Scientific) was added. The tube was incubated at 37°C for 60 min, then 40 mM iodoacetamide (IAM, Sigma) was added and mixed for 40 min in the dark. Cold acetone (acetone/sample, v/v, 6/1) was added to the tube to precipitate proteins at −20°C for 4 h. After centrifugation at 10 000 × *g* for 20 min at 4°C, the supernatant was discarded. The pellet was dissolved in 100 µl of 100 mM triethylammonium bicarbonate (TEAB) (Sigma). Finally, protein was digested with trypsin (trypsin/sample, w/w, 1/25) at 37°C overnight. Following trypsin digestion, peptides were dried using a vacuum centrifugal pump.

Peptides were reconstituted in 400 mM TEAB and labeled using 8-plex iTRAQ reagents (Sciex) according to the manufacturer's instructions. The 3 replicates of planktonic cells (PL1, PL2, and PL3) were labeled using the iTRAQ tags 113, 114, and 115, respectively. The 3 replicates of attached cells (AT1, AT2, and AT3) were labeled using the iTRAQ tags 116, 117, and 118 respectively. After 2 h of culture at room temperature, the labeled groups were mixed and dried under a vacuum.

2.7. LC-MS/MS analysis

The iTRAQ-labeled peptides were separated into 2 dimensions, with high pH in the first dimension for the C18 reverse-phase HPLC (high performance liquid chromatography) column and acidic pH in the second dimension (Gilar et al. 2005, Dwivedi et al. 2008, Yang et al. 2012). The peptide samples were reconstituted with 100 µl buffer (2% acetonitrile (Thermo Fisher Scientific), pH adjusted to 10 with ammonia) and separated with a C18 column (1.7 µm, 3 × 150 mm; Waters) using ACQUITY ultra performance liquid chromatography (UPLC) equipped with UV detection (Waters). The eluted phases consisted of an A phase (2% acetonitrile, pH 10) and a B phase (80% acetonitrile, pH 10). Peptides were eluted with a variable gradient of solvent B from 3.8 to 100% B over 66 min at a flow rate of 400 µl min^{-1}.

Elution was monitored by measuring the absorbance at 214 nm, and fractions were collected every minute. The eluted peptides were pooled into 10 different fractions and vacuum dried.

Each of the 10 dried fractions was resuspended in buffer (2% acetonitrile, 0.1% formic acid). The fractions were further separated using a Q-exactive mass spectrometer (Thermo Fisher Scientific) coupled with an EASY-nLC 1200 liquid chromatography system (Thermo Fisher Scientific). For liquid chromatography, fractions were separated using a C18 column (75 µm × 25 cm, Thermo Fisher Scientific) using 2% acetonitrile with 0.1% formic acid (A phase, Thermo Fisher Scientific) and 80% acetonitrile with 0.1% formic acid (B phase) as eluent from 5 to 100% B over 120 min at a flow rate of 300 nl min^{-1}. The mass spectrometer was set to perform data-dependent acquisition (DDA) with a selected mass range of 350–1300 *m/z*. The 20 parent ions with the strongest signals were selected for secondary fragmentation.

2.8. Database search and bioinformatic analysis

MS/MS spectra were analyzed using a MASCOT engine embedded into Proteome Discoverer 2.1 (Thermo Fisher Scientific) against the data from *Pseudoalteromonas* (229 065 sequences downloaded on March 23, 2017) from the Uniprot database. For protein identification, the following options were used. A mass tolerance of 10 ppm for precursor ions and 0.05 Da for fragmented ions was specified. The cleavage enzyme was defined as trypsin and was allowed up to 2 miscleavages. Carbamidomethylation on cysteine, iTRAQ8plex (K), and iTRAQ8plex (N-term) were set as fixed modifications, while oxidation (M), acetyl (Protein N-Terminus), and iTRAQ-8plex (Y) were defined as variable modifications. The estimated false discovery rate was specified at a maximum of 1% for both peptide and protein identification, and the peptide ion score was set to >20. Differentially expressed proteins (DEPs) were identified only if the p-value was lower than 0.05 (statistically analyzed by a paired *t*-test) and fold change (FC) was higher than 1.5 (up-regulated) or lower than 0.67 (down-regulated) between the 2 groups. Functional annotations and classification of DEPs were carried out using Gene Ontology (GO; www.geneontology.org). GO has 3 ontologies describing molecular functions, cellular components, and biological processes. The Kyoto encyclopedia of genes and genomes (KEGG; www.kegg.jp) was employed to identify major metabolic pathways affected by the planktonic to sessile transition. Statistically significant enrichments were identified as those with a p-value less than 0.05 using Fisher's exact test. Hierarchical clustering analysis was conducted using Cluster 3.0 software.

2.9. RNA extraction and quantitative real-time PCR

To evaluate the correlation between protein abundance and mRNA expression, quantitative real-time PCR (qRT-PCR) was used to determine expression levels of mRNA. To provide further validation of DEP identification, the mRNA expression patterns of 3 genes for which protein expression was down-regulated (AcrB, CPB, and SecF) and 2 genes for which protein expression was up-regulated (E-F and FtsY) were investigated using qRT-PCR. Total RNA was extracted from planktonic and attached *Pseudoalteromonas* sp. W-7 using RNAiso plus (TaKaRa) following the manufacturer's instructions. The extracted RNA was treated with RNase-free DNase (Promega) to eliminate any DNA contamination. RNA quality was checked by agarose gel electrophoresis. Synthesis of cDNA was conducted using a PrimeScript™ RT reagent kit (TaKaRa). An ABI™ 7500 real-time PCR system (Applied Biosystems) was used for gene expression analysis of target genes using SYBR green qPCR master mix primers (Vazyme) (Table 1) with the following settings: initial denaturation at 95°C for 5 min, followed by 40 cycles of 95°C for 15 s and 60°C for 1 min. Samples for qRT-PCR were run in 3 replicates. Melting curve analysis was performed to verify the specificity of PCR products. Data were normalized using the 16S rRNA gene as an internal control, and the relative expression levels of target genes were calculated through the $2^{-\Delta\Delta Ct}$ method.

2.10. Statistical analysis

For the assay to evaluate attachment capacity, the assay to obtain initially adhered bacterial cells that had not yet replicated, and qRT-PCR, statistical analyses were performed using SPSS 22.0 software. The data were tested for normality using the Kolmogorov–Smirnov test and for homogeneity of variance using Levene's test. Since the assumptions of normality and homogeneity of variance were met, a 1-way ANOVA was applied followed by Tukey's post-hoc test. The significance level was defined as $p < 0.05$.

Table 1. Details of primers used for qRT-PCR

Gene	Sequences (5'–3')	Description
E-F (forward)	AGT TCA AGG GCG GCC TAA AA	Elongation factor P
E-F (reverse)	ATG CCA AAA TTC GCC GTC TG	
FtsY (forward)	TTG CCG TTG CTG ATA AGT T	Signal recognition particle receptor FtsY
FtsY (reverse)	GCT CTT GAA GGT GCG TAA	
AcrB (forward)	GAT GGC TAC TCG TAT GAT GAA	Multidrug transporter AcrB
AcrB (reverse)	TTA CTT GTG GCT GCT GTT	
CPB (forward)	ACT AGC CTT GAC GAA CTG CC	Capsular polysaccharide biosynthesis protein
CPB (reverse)	TGT GCC CAA CCG GTA ATA CC	
SecF (forward)	CCC TCG CGG TGA TGA TGT AA	Protein-export membrane protein SecF
SecF (reverse)	CGC AGT TAA CAT GGC AAG GC	
16S rRNA (forward)	AGC ACC TGT ATC AGA GTT	16S rRNA
16S rRNA (reverse)	AAG AAC CTT ACC TAC ACT TG	

3. RESULTS

3.1. Strain identification and attachment of marine bacteria

The 16S rRNA gene analysis of the 51 isolated strains identified 28 genera (Table 2). Eleven strains were classified as relatively strong biofilm formers: W-1 (*Leisingera* sp.), W-2 (*Roseobacter* sp.), W-7 (*Pseudoalteromonas* sp.), W-8 (*Alteromonas* sp.), D-1 (*Tenacibaculum discolor*), D-2 (*Vibrio parahaemolyticus*), D-6 (*Tenacibaculum mesophilum*), Y-5 (*Pseudoalteromonas* sp.), Y-9 (*Chryseobacterium* sp.), Y-15 (*Aquimarina* sp.), and Y-19 (*Acinetobacter* sp.).

Fig. 1 shows the density of attached bacteria after a 3 h culture of the initial bacterial suspension (10^7 cells ml^{-1}) for 6 strains (W-7, D-1, D-2, D-6, Y-5, and Y-19). There were significant differences in the density of attached bacteria between these strains ($p < 0.05$, Fig. 1). *Pseudoalteromonas* sp. strain W-7 showed the highest density of attached cells, suggesting that this strain has an efficient and rapid attachment mechanism. Due to the relatively strong biofilm-forming (Table 2) and attachment capacity (Fig. 1) exhibited by *Pseudoalteromonas* sp. W-7, this strain was chosen for further study.

3.2. Initial adhesion of *Pseudoalteromonas* sp. strain W-7

For strain W-7, the density of cells attached to coverslips after 1 h in cell suspension was not significantly different from that of cells further cultured in FSW for 2 h ($p = 0.898$). This indicates that most bacterial cells did not divide during the first 3 h of adhesion (Fig. 2). When bacterial cells that attached during the first 1 h were cultured for a further 4 h, the cell density increased significantly ($p = 0.03$). The cell density continued to increase when the bacterial cells were cultured longer, indicating cell division (Fig. 2). These results indicate that during the first 3 h of adhesion of *Pseudoalteromonas* sp. W-7, the bacterial cells transitioned from the planktonic to the sessile state without significant cell division.

3.3. Protein identification and annotation of DEPs

A total of 3468 proteins were identified (see Figs. S1–S3 and Texts S1–S3 in the Supplement at www.int-res.com/articles/suppl/a086p069_supp.pdf).

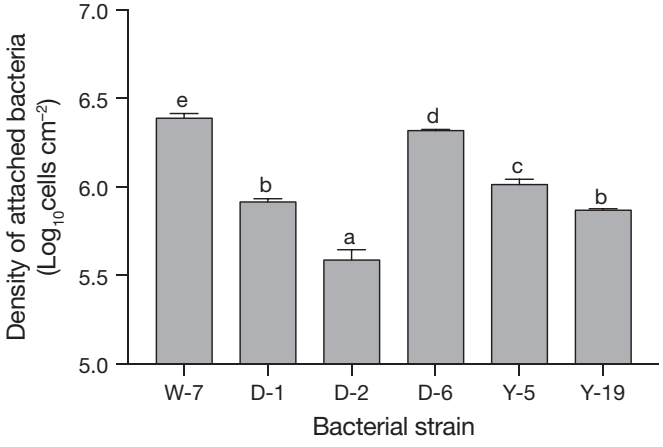

Fig. 1. Density of attached bacteria after a 3 h culture of the initial bacterial suspension. W-7: the strain *Pseudoalteromonas* sp. W-7; D-1: the strain *Tenacibaculum discolor* D-1; D-2: *Vibrio parahaemolyticus* D-2; D-6: *Tenacibaculum mesophilum* D-6; Y-5: *Pseudoalteromonas* sp. Y-5; Y-19: *Acinetobacter* sp. Y-19. There were 3 replicates for each strain. Error bars show standard deviation. Letters denote significant differences among strains ($p < 0.05$, 1-way ANOVA)

Table 2. Isolated bacterial strains and their biofilm-forming capacity. Strains isolated from epoxy panels submerged near Dalipuyu Islet, China, are indicated by W, strains isolated from glass slides submerged near Dongshan Island, China, are indicated by D, and strains isolated from the bridge pillar of the Yanwu Bridge, China, are indicated by Y. Accession numbers correspond to the sequences from the best hit database for each strain. Strains were considered to have relatively strong biofilm-forming capacity when crystal violet absorbance $OD_{600} > 0.8$

Strain	Reported strain with maximum similarity	Accession number	Identity (%)	OD_{600} for biofilm (mean ± SD)
W-8	*Alteromonas* sp.	HQ012269.1	99	3.764 ± 0.033
D-2	*Vibrio parahaemolyticus*	KR347245.1	100	2.135 ± 0.132
W-7	*Pseudoalteromonas* sp.	FJ695538.1	99	2.068 ± 0.048
Y-15	*Aquimarina* sp.	JN207970.1	99	2.033 ± 0.275
W-2	*Roseobacter* sp.	FM180521.1	99	1.898 ± 0.231
D-6	*Tenacibaculum mesophilum*	NR113841.1	100	1.449 ± 0.120
Y-19	*Acinetobacter* sp.	JF411429.1	99	1.243 ± 0.098
Y-9	*Chryseobacterium* sp.	GQ359994.1	99	1.095 ± 0.070
Y-5	*Pseudoalteromonas* sp.	FJ169963.1	99	1.067 ± 0.106
W-1	*Leisingera* sp.	EF574305.1	99	1.043 ± 0.185
D-1	*Tenacibaculum discolor*	JQ231116.1	99	0.808 ± 0.077
D-11	*Labrenzia* sp.	KP301106.1	99	0.771 ± 0.045
Y-16	*Ascidiimonas* sp.	LC066536.1	100	0.688 ± 0.019
Y-8	*Phaeobacter* sp.	KJ205616.1	100	0.642 ± 0.072
D-18	*Halobacillus* sp.	KF933611.1	100	0.437 ± 0.043
D-13	*Microbulbifer variabilis*	JN128259.1	99	0.396 ± 0.017
D-16	*Vibrio alginolyticus*	KT986145.1	100	0.347 ± 0.045
D-7	*Vibrio azureus*	HM032017.1	99	0.313 ± 0.045
D-5	*Tenacibaculum holothuriorum*	KP313827.1	97	0.313 ± 0.034
D-9	*Bacillus hwajinpoensis*	HE662818.1	99	0.268 ± 0.025
D-12	*Vibrio parahaemolyticus*	KX035060.1	100	0.244 ± 0.073
W-6	*Tenacibaculum* sp.	KM047889.1	98	0.234 ± 0.033
W-3	*Marinomonas* sp.	DQ480145.1	99	0.232 ± 0.042
D-3	*Erythrobacter nanhaisediminis*	KJ009560.1	99	0.193 ± 0.140
D-10	*Marinobacter hydrocarbonoclasticus*	KF052990.1	100	0.174 ± 0.006
D-8	*Vibrio crassostreae*	KR347208.1	99	0.154 ± 0.006
D-21	*Pseudomonas* sp.	KU643205.1	99	0.147 ± 0.060
W-5	*Bacillus* sp.	KX817960.1	100	0.135 ± 0.005
Y-12	*Vibrio alginolyticus*	KT986145.1	100	0.129 ± 0.004
W-4	*Tenacibaculum litoreum*	KJ009531.1	99	0.128 ± 0.007
Y-11	*Pseudomonas* sp.	AB681548.1	99	0.119 ± 0.003
Y-18	*Rhodovulum sulfidophilum*	CP015421.1	99	0.116 ± 0.028
D-19	*Oceanisphaera* sp.	KU985333.1	99	0.116 ± 0.021
D-23	*Vibrio harveyi*	KC884637.1	99	0.116 ± 0.004
D-14	*Galbibacter* sp.	KC121350.1	99	0.114 ± 0.009
Y-10	*Bacillus thuringiensis*	KU179338.1	100	0.114 ± 0.004
D-15	*Bacillus* sp.	KX817930.1	100	0.113 ± 0.004
D-22	*Vibrio* sp.	EF187016.1	100	0.113 ± 0.004
D-17	*Pseudoalteromonas spongiae*	KM041227.1	99	0.109 ± 0.004
Y-17	*Tenacibaculum lutimaris*	JN128277.1	99	0.108 ± 0.005
D-4	*Bacillus megaterium*	KU161279.1	100	0.103 ± 0.005
Y-2	*Tenacibaculum* sp.	JF895523.1	99	0.102 ± 0.001
D-20	*Halomonas* sp.	KJ188001.1	97	0.101 ± 0.008
Y-3	*Bacillus cereus*	KP985690.1	100	0.097 ± 0.008
Y-4	*Enterobacter hormaechei*	KJ863539.1	99	0.096 ± 0.023
Y-1	*Algoriphagus halophilus*	AY264839.2	99	0.092 ± 0.002
Y-7	*Polaribacter* sp.	KT121443.1	97	0.088 ± 0.005
Y-14	*Flavobacterium dongtanense*	GU073292.1	99	0.087 ± 0.002
Y-6	*Bacillus* sp.	KX817934.1	100	0.084 ± 0.010
Y-20	*Cyclobacterium* sp.	AJ244689.1	99	0.083 ± 0.009
Y-13	*Agrococcus* sp.	KJ191076.1	99	0.083 ± 0.002
Control	Without bacterial cells	/	/	0.054 ± 0.002

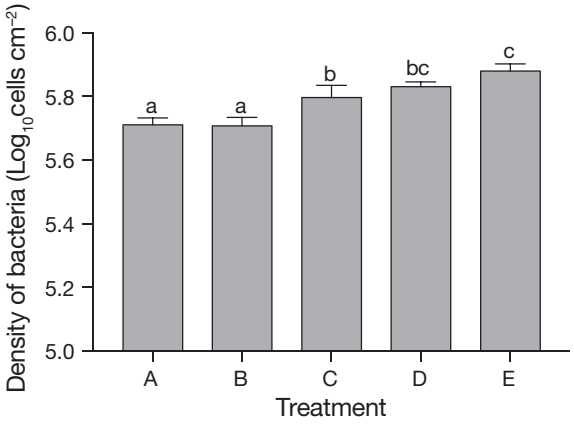

Fig. 2. Cell density of attached *Pseudoalteromonas* sp. W-7 after 1 h and with subsequent increases in culture time of 2, 4, 6, and 8 h. Treatment A: density of attached cells after 1 h; Treatment B: density of attached cells after 1 h of attachment and further incubation for 2 h; Treatment C: density of attached cells after 1 h of attachment and further incubation for 4 h; Treatment D: density of attached cells after 1 h of attachment and further incubation for 6 h; and Treatment E: density of attached cells after 1 h of attachment and further incubation for 8 h. There were 3 replicates for each treatment. Error bars show standard deviation. Letters denote significant differences among treatments ($p < 0.05$, 1-way ANOVA)

There were 163 DEPs identified between planktonic cells and attached cells: 120 proteins were down-regulated and 43 proteins were up-regulated in attached cells relative to planktonic cells. Table 3 lists the information of the 163 differentially expressed proteins identified in planktonic and attached cells, including UniProt accession number, protein name, fold change, p-value and direction of regulation. Clustering results indicated that DEPs were divided into 2 modules (see Fig. S4 in the Supplemen). In module 1, 43 DEPs showed up-regulated expression patterns in replicates of AT relative to replicates of PL. In module 2, 120 DEPs showed down-regulated expression patterns in replicates of AT relative to replicates of PL.

3.4. GO and KEGG analysis of DEPs

Fig. 3 shows the GO annotation analysis of up-regulated and down-regulated proteins. In terms of biological processes, DEPs were mainly involved in cellular processes, metabolic processes, and localization. In terms of cellular components, DEPs were mainly distributed in the categories of cell part, membrane part, and membrane. In terms of molecular function, DEPs were mainly involved in binding, catalytic activity, and transporter activity. We annotated the identified DEPs using the KEGG database; all mapped onto 10 KEGG pathways, of which pyruvate metabolism, carbon fixation pathway in prokaryotes, and carbon metabolism were significantly affected (Fig. 4).

3.5. Validation of DEPs by qRT-PCR analysis

The expression patterns of E-F, AcrB, CPB, and SecF were consistent with patterns obtained by iTRAQ analysis (Fig. 5). However, the mRNA expression level of FtsY did not differ significantly between AT and PL, contrasting with patterns of protein expression for this gene and suggesting that protein levels may be determined not only at the transcription level but also at the post-translational level.

4. DISCUSSION

Pseudoalteromonas sp. strain W-7 produced biofilms in marine broth and rapidly attached to glass slides. Members of the genus *Pseudoalteromonas* are recognized as marine biofilm formers and are commonly found colonizing various marine surfaces (Rao et al. 2005, Saravanan et al. 2006, Bowman 2007, Favre et al. 2018). *Pseudoalteromonas* species have been shown to produce many bioactive natural products, and appear to play significant ecological roles (Bowman 2007). Biofilms formed by *Pseudoalteromonas* species can affect the settlement and metamorphosis of many invertebrates as well as the settlement of macroalgae (Holmström et al. 2002, Huggett et al. 2006, Huang et al. 2007, Zeng et al. 2015, 2017). For example, *P. luteoviolacea* induced larval metamorphosis of the marine tubeworm *Hydroides elegans* (Shikuma et al. 2014). *P. tunicata*, originally isolated from the surface of a tunicate, was found to possess a broad range of antifouling capabilities against invertebrate larvae and algal spores (Holmström et al. 1998, Egan et al. 2002). Given the ecological significance of *Pseudoalteromonas*, this genus appears to be a good model organism for the study of attachment mechanisms among marine bacteria.

In the present study, good biofilm-forming capacity was also observed in 8 other genera, among which *Leisingera*, *Roseobacter*, *Alteromonas*, *Tenacibaculum*, *Vibrio*, *Chryseobacterium*, and *Acinetobacter* had been previously reported to be capable of forming biofilms or had been found in biofilms (Huang et

Table 3. The 163 differentially expressed proteins (DEPs) identified in planktonic (PL) and attached (AT) cells

UniProt accession number	Protein name	Fold change (AT/PL)	p-value (AT/PL)	Direction of regulation
A0A0P9G3Q4	Bicarbonate transporter BicA	0.29	0.0011	Down
A0A1L6KW31	Integrase	0.31	0.0026	Down
A0A099LGG3	Citrate transporter	0.34	0.0011	Down
A0A0U2V454	Uncharacterized protein	0.39	0.0061	Down
A0A0U2ISG6	Uncharacterized protein	0.39	0.0008	Down
A0A0U2WYP9	Uncharacterized protein	0.39	0.0008	Down
A0A0W1LFC4	Sulfate permease	0.40	0.0074	Down
A0A0U2NG71	Uncharacterized protein	0.41	0.0003	Down
A0A0W1L7N9	Uncharacterized protein	0.41	0.0019	Down
A0A0Q0G6G6	Cytochrome bo(3) ubiquinol oxidase subunit 1	0.42	<0.0001	Down
A0A0S2K0E9	Haloacid dehalogenase	0.42	0.0030	Down
U1KEH0	ATP synthase subunit alpha	0.42	0.0034	Down
A0A099L9V1	Amino acid carrier protein	0.43	0.0068	Down
A0A099L635	Uncharacterized protein	0.43	0.0064	Down
A0A099LJD7	Uncharacterized protein	0.43	0.0002	Down
A0A1E3X0L0	Cytochrome d terminal oxidase subunit 10	0.44	0.0003	Down
A0A0U2VH09	Uncharacterized protein	0.44	0.0054	Down
A0A0U2WYR4	Uncharacterized protein	0.45	0.0005	Down
A0A0W1L7N2	Nucleoside-diphosphate sugar epimerase	0.45	<0.0001	Down
A0A099LBW0	Sodium:dicarboxylate symporter	0.46	0.0012	Down
N6UYQ8	Uncharacterized protein	0.46	0.0145	Down
A0A0U2V4M2	Uncharacterized protein	0.46	0.0003	Down
A0A1E3WZB0	Multidrug transporter AcrB	0.47	0.0005	Down
A0A0Q0IW23	Cytochrome b	0.47	0.0017	Down
A0A0B2JQA6	Phospho-N-acetylmuramoyl-pentapeptide-transferase	0.47	0.0075	Down
G7ESH9	Uncharacterized protein	0.47	0.0006	Down
A0A1E3WWD7	O-antigen polymerase	0.48	0.0040	Down
G7ESI2	Uncharacterized protein	0.48	0.0050	Down
A0A1E3WUA8	Aminobenzoyl-glutamate transporter	0.48	0.0012	Down
A0A063KRR1	Guanine permease	0.48	0.0040	Down
A0A0N8TWS8	Sodium:neurotransmitter symporter family protein	0.49	0.0020	Down
A0A0S3AV43	Uncharacterized protein	0.50	0.0010	Down
A0A063KQ81	MFS transporter	0.50	0.0029	Down
A0A099LGK9	Subtilisin, Xanthomonalisin	0.50	0.0025	Down
A0A0N1EMB9	Sodium:proton antiporter	0.50	0.0009	Down
A0A0P7DZ52	Uncharacterized protein	0.50	0.0165	Down
A0A099LG56	Nucleoside permease	0.51	0.0049	Down
E6RM70	Uncharacterized protein	0.51	0.0024	Down
A0A099L933	Uncharacterized protein	0.51	0.0031	Down
A0A0U2WWT5	Uncharacterized protein	0.51	0.0022	Down
A0A063KIN6	ABC transporter permease	0.52	0.0032	Down
A0A0U2X1W8	Uncharacterized protein	0.52	0.0119	Down
A0A0B2JA34	DNA-directed DNA polymerase	0.52	0.0003	Down
A0A0S3AZJ2	Putative permease	0.52	0.0042	Down
A0A0W1L7G3	Major capsid protein	0.52	0.0040	Down
A0A099L726	Uncharacterized protein	0.53	0.0066	Down
A0A0U2VH29	Uncharacterized protein	0.53	0.0040	Down
A0A0U2WLH0	Uncharacterized protein	0.53	0.0020	Down
Z9JZE0	Ktr system potassium transporter B	0.54	0.0008	Down
A0A0W1L719	Terminase	0.54	0.0100	Down
A0A0S3ATD7	Capsular polysaccharide biosynthesis protein	0.54	0.0088	Down
A0A099LH05	Sulfate transporter	0.55	0.0003	Down
A0A063KTZ3	Sodium:dicarboxylate symporter	0.55	0.0005	Down
A0A167LQZ7	Uncharacterized protein	0.55	0.0201	Down
A0A0U2LME9	Uncharacterized protein	0.55	0.0003	Down
A0A099L4K1	Magnesium transporter MgtE	0.55	<0.0001	Down
A0A0W1L6F5	Uncharacterized protein	0.56	0.0104	Down
A0A099LFD0	Polysaccharide biosynthesis protein	0.56	0.0377	Down
A0A1N6EPP6	MFS transporter, SP family, sugar:H+ symporter	0.56	<0.0001	Down

Table 3 (continued)

UniProt accession number	Protein name	Fold change (AT/PL)	p-value (AT/PL)	Direction of regulation
A0A0Q0IBU0	Small-conductance mechanosensitive channel	0.56	0.0009	Down
A0A1E3WTQ8	Nucleoside-diphosphate sugar epimerase	0.56	0.0024	Down
E6RM02	TPR repeat-containing protein	0.56	0.0008	Down
A0A0W1L5E7	Uncharacterized protein	0.57	0.0068	Down
A0A099LD26	Tryptophan/tyrosine permease	0.57	0.0111	Down
A0A099L8Y7	Amino acid/peptide transporter	0.57	0.0029	Down
A0A0Q0ITZ0	Nucleoside recognition	0.58	0.0049	Down
A0A099L5T9	Probable peptidoglycan glycosyltransferase FtsW	0.58	0.0052	Down
A0A063KSN1	Membrane protein	0.58	0.0035	Down
A0A0U2WHI7	Uncharacterized protein	0.58	0.0129	Down
N6V9K2	Uncharacterized protein	0.58	0.0163	Down
G7EVS5	Lipopolysaccharide biosynthesis protein	0.59	0.0048	Down
A0A099LD40	Protein-export membrane protein SecF	0.59	0.0005	Down
A0A099LFA9	DNA repair protein RecN	0.59	0.0087	Down
A0A167ENQ6	DNA-directed RNA polymerase subunit beta	0.59	0.0013	Down
A0A099LA70	Uncharacterized protein	0.60	0.0003	Down
Z9JZN0	Peptidyl-tRNA hydrolase	0.60	0.0117	Down
A0A099LHD3	Uncharacterized protein	0.60	0.0111	Down
A0A0W1LAY6	Protein Xni	0.61	0.0164	Down
A0A0Q0IFK4	Uncharacterized protein	0.61	0.0100	Down
A0A099LFU3	Ion transport protein	0.61	0.0087	Down
A0A0P7E133	Ligand-gated channel protein	0.61	0.0027	Down
A0A0M9UHL3	Outer membrane protein assembly factor BamD	0.61	0.0006	Down
A0A0Q0H272	Major outer membrane protein P.IB	0.61	0.0009	Down
A0A1E3X1K4	Multidrug transporter AcrB	0.61	0.0034	Down
A0A0U2WCG1	Uncharacterized protein	0.62	0.0003	Down
Z9K5U1	Thiol:disulfide interchange protein DsbD	0.62	0.0005	Down
A0A0P7DAB2	Poly(A) polymerase I	0.63	0.0293	Down
A0A0U2WHL8	Uncharacterized protein	0.63	0.0382	Down
F3BGV3	DNA-directed RNA polymerase subunit beta	0.63	0.0007	Down
Z9K579	2,3,4,5-tetrahydropyridine-2,6-carboxylate N-succinyltransferase	0.63	0.0177	Down
A0A1N6DRX0	Tyrosine-specific transport protein	0.63	0.0003	Down
A0A0S3ARN0	Multidrug resistance protein(AcrB/AcrD/AcrF)	0.63	0.0299	Down
A0A0P9GDG4	Uncharacterized protein	0.63	0.0020	Down
G7F5H8	Curli production assembly/transport component CsgF	0.63	0.0169	Down
A0A0S3AV96	Membrane protein	0.64	0.0106	Down
A0A0W1KPX5	Carbon starvation protein CstA	0.64	0.0196	Down
A0A0S3ATM1	Multidrug ABC transporter ATP-binding protein	0.64	0.0004	Down
N6V2T5	Uncharacterized protein	0.64	0.0157	Down
G7EVS2	Uncharacterized protein	0.64	0.0225	Down
A0A1E3WWI1	Amidohydrolase	0.64	0.0043	Down
Z9K4D0	DNA-directed RNA polymerase subunit beta	0.64	0.0002	Down
E6RQT4	Putative secreted major subunit of curlin	0.64	0.0073	Down
Z9K1Z5	Ankyrin	0.64	0.0029	Down
G7ETU6	AcrB/AcrD/AcrF family metabolite exporter	0.65	0.0042	Down
A0A0B2JJA4	Cytochrome C peroxidase	0.65	0.0033	Down
G7EVS1	Small conductance mechanosensitive channel	0.65	0.0026	Down
A0A099LM11	Uncharacterized protein	0.65	0.0009	Down
A0A063KPA1	Na(+)-translocating NADH-quinone reductase subunit E	0.65	0.0212	Down
A0A0Q0NI48	ATP synthase subunit a	0.65	0.0060	Down
Z5XQD0	TonB-dependent receptor	0.65	0.0358	Down
E6RP68	Sodium/proline symporter	0.66	0.0058	Down
A0A099L8H2	Uncharacterized protein	0.66	0.0126	Down
Z9K4P6	General secretion pathway protein GspD	0.66	0.0032	Down
A0A0S3AUA5	RND transporter	0.66	0.0008	Down
U1KTF0	Aminotransferase	0.66	0.0122	Down
Z9K1N4	Capsular biosynthesis protein	0.66	0.0143	Down
A0A0U2VGZ7	Uncharacterized protein	0.66	0.0196	Down

Table 3 (continued)

UniProt accession number	Protein name	Fold change (AT/PL)	p-value (AT/PL)	Direction of regulation
A0A099L7R7	Uncharacterized protein	0.66	0.0011	Down
A0A0F4NVK3	Na(+)-translocating NADH-quinone reductase subunit B	0.66	0.0170	Down
A0A099LBE5	Di-heme cytochrome, transmembrane	0.66	0.0067	Down
Z9K0A5	Imidazoleglycerol-phosphate dehydratase	1.51	<0.0001	Up
A0A0W1KXG3	Acetylornithine aminotransferase	1.52	0.0290	Up
A0A0F4QZ24	Succinate-CoA ligase	1.52	0.0023	Up
A0A1E3X1L8	ATP synthase epsilon chain	1.52	0.0144	Up
G7F5U0	50S ribosomal protein	1.52	0.0084	Up
L8CZA1	50S ribosomal protein	1.52	0.0006	Up
A0A0F4PS78	Protein RecA	1.53	0.0097	Up
Q15YI8	Acetyl-coenzyme A synthetase	1.53	0.0109	Up
V4HPA9	Uncharacterized protein	1.54	0.0096	Up
A0A166X2A8	Imidazoleglycerol-phosphate dehydratase	1.54	0.0013	Up
A0A0P9FU25	Sensor histidine kinase YpdA	1.56	0.0029	Up
G7EWH6	30S ribosomal protein	1.56	0.0021	Up
G7EQL9	Probable sigma(54) modulation protein	1.56	0.0158	Up
V4HKR1	Uncharacterized protein	1.56	0.0026	Up
A4CCV3	Small heat shock protein	1.57	0.0001	Up
A0A1E2TIE9	3-ketoacyl-CoA thiolase	1.59	0.0157	Up
A0A0Q0NNR0	Malonyl CoA-acyl carrier protein transacylase	1.60	0.0006	Up
Z9K4Q6	Phage-shock protein	1.60	0.0037	Up
U1MD60	UPF0234 protein	1.62	0.0237	Up
A0A0W1KR13	50S ribosomal protein	1.62	0.0109	Up
A0A0S3AY85	Enolase-phosphatase E1	1.63	0.0038	Up
A0A0U2NFD1	Polyribonucleotide nucleotidyltransferase	1.64	0.0075	Up
A0A1E3WVT0	ATP phosphoribosyltransferase	1.64	<0.0001	Up
A0A0S3AQG3	50S ribosomal protein	1.64	0.0140	Up
A0A0Q0GTM4	50S ribosomal protein	1.66	0.0227	Up
A0A0F4QVV1	Succinate-CoA ligase [ADP-forming] subunit beta	1.66	0.0042	Up
A0A0L0EMP6	Uncharacterized protein	1.70	0.0340	Up
A0A1N6GH09	LSU ribosomal protein L13P	1.75	0.0042	Up
A0A0Q0GJD3	Manganese-dependent inorganic pyrophosphatase	1.78	0.0103	Up
A0A063KKW1	Elongation factor P	1.80	0.0115	Up
A0A0S3ATH8	Ribonuclease E	1.80	0.0043	Up
A0A0Q0ICZ7	UTP-glucose-1-phosphate uridylyltransferase	1.81	0.0048	Up
U1LYU5	DNA-directed RNA polymerase subunit omega	1.93	0.0177	Up
Z9K4T0	50S ribosomal protein	1.94	0.0019	Up
A4CEF5	Uncharacterized protein	2.03	0.0003	Up
A0A099LAZ1	Uncharacterized protein	2.04	0.0001	Up
A0A0W1L519	Enoyl-CoA hydratase	2.15	0.0002	Up
Z9K8D5	Acetyltransferase component of pyruvate dehydrogenase complex	2.16	0.0016	Up
A0A1E3WV66	Signal recognition particle receptor FtsY	2.20	0.0015	Up
A0A0Q0IZD8	30S ribosomal protein S17	2.27	0.0044	Up
A0A1N6FNJ2	LSU ribosomal protein L22P	2.33	0.0023	Up
A0A0W1L143	UTP-glucose-1-phosphate uridylyltransferase	2.80	0.0009	Up
A0A0S3AWJ6	Membrane protein	5.06	<0.0001	Up

al. 2008, Vandecandelaere et al. 2008, Gaddy et al. 2009, Yildiz & Visick 2009, Lin et al. 2010, Romero et al. 2010, Elifantz et al. 2013, Yang et al. 2016a). To our knowledge, the present study is the first to report strong biofilm-forming capacity in the genus *Aquimarina*. In terms of bacterial attachment, the strain *Tenacibaculum mesophilum* D-6 also exhibited rapid attachment in the present study, with the density of attached cells after 3 h of culture the second highest among the 6 strains tested. To date, there is little information on attachment in the genus *Tenacibaculum*, although members of this genus have been found in marine biofilms (Yang et al. 2016a,b). *T. mesophilum* D-6 might therefore be a useful strain for further studies of this genus. It should also be noted that different strains from the same genus

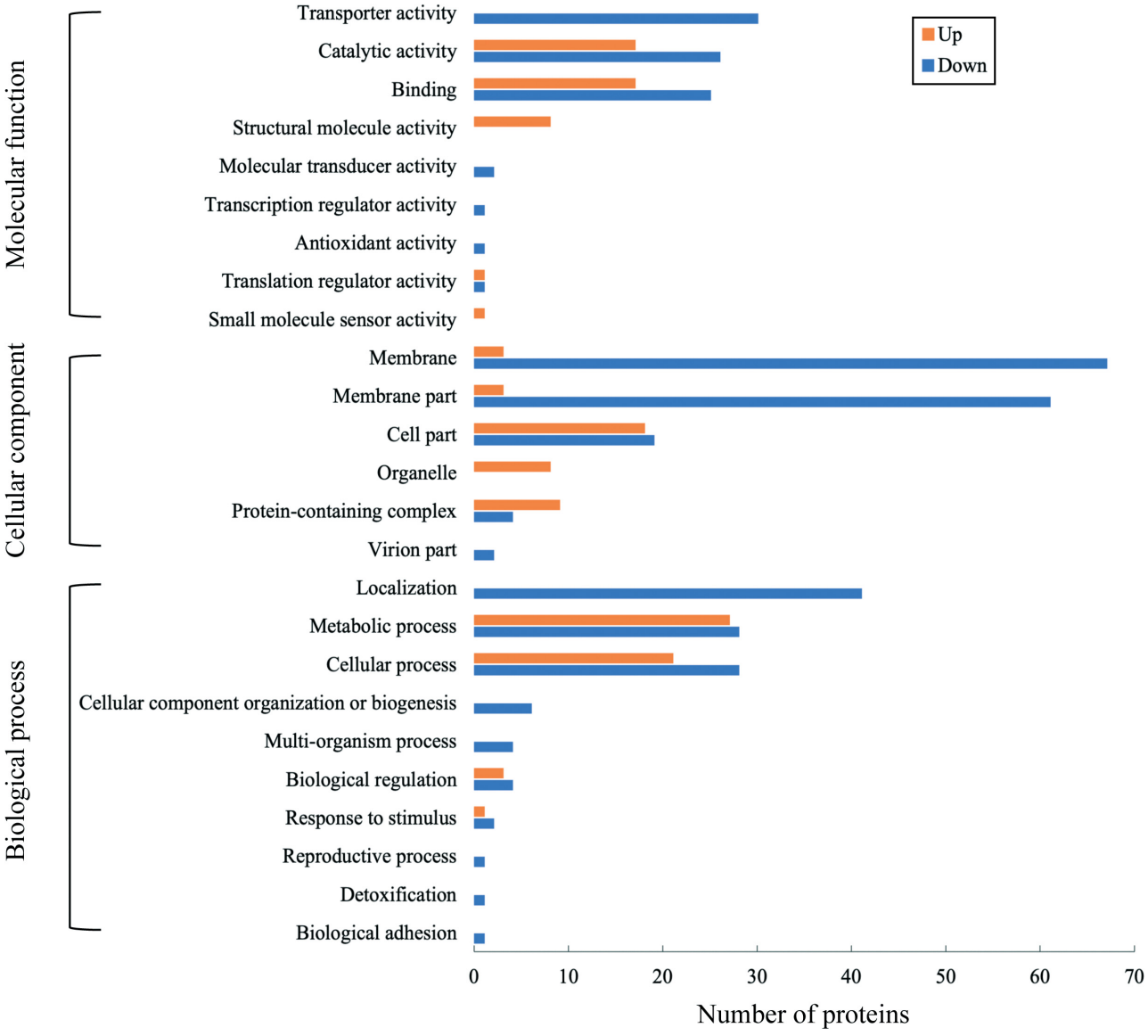

Fig. 3. Gene ontology (GO) annotation analysis of differentially expressed proteins. Up and Down: proteins that are up- and down-regulated, respectively, in attached cells relative to planktonic cells

showed different biofilm formation ability in some cases. For example, different strains of *Tenacibaculum* showed variable biofilm-forming capacity, with the OD_{600} varying from 0.102 (*Tenacibaculum* sp. Y-2) to 1.449 (*T. mesophilum* D-6) (Table 2), indicating that biofilm formation ability of bacteria is strain-specific. Future studies could focus on strains that share similar genotypes but vary in biofilm formation ability to investigate the causes of this variability.

Our results indicated that expression of the acetyltransferase component of the pyruvate dehydrogenase complex was significantly up-regulated in initially adherent cells of *Pseudoalteromonas* sp. strain W-7 compared to planktonic cells (AT/PL = 2.16). The acetyltransferase component of the pyruvate dehydrogenase complex can catalyze the oxidative decarboxylation of pyruvate to acetyl-CoA, which plays an important role in energy metabolism. Furthermore, acetyl-coenzyme A synthetase expression was also significantly up-regulated in initially adherent cells of strain W-7 (AT/PL = 1.53); this enzyme also maps on to pyruvate metabolism and carbon metabolism pathways based on KEGG analysis, indicating that pyruvate metabolism and carbon metabolism might play important roles in the attachment of *Pseudoalteromonas* sp. W-7. Acetyl-coenzyme A synthetase has been reported to be important for bacterial growth in *Pseudomonas putida* U (Arias-Barrau et al. 2006). In a study by

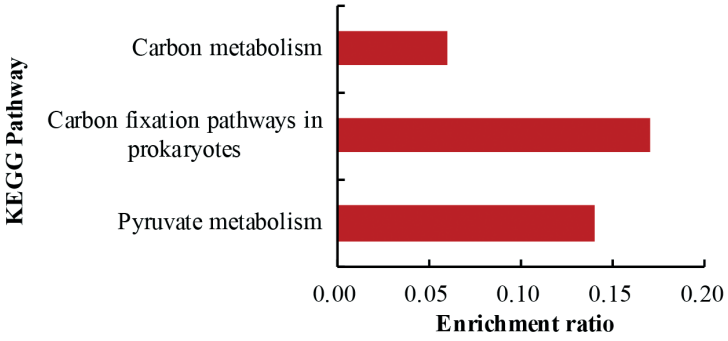

Fig. 4. Kyoto encyclopedia of genes and genomes (KEGG) pathway enrichment analysis of differentially expressed proteins (DEPs) for the planktonic to sessile transition. The enrichment ratio is defined as the ratio of the number of DEPs in the pathway to the total number of proteins in the pathway

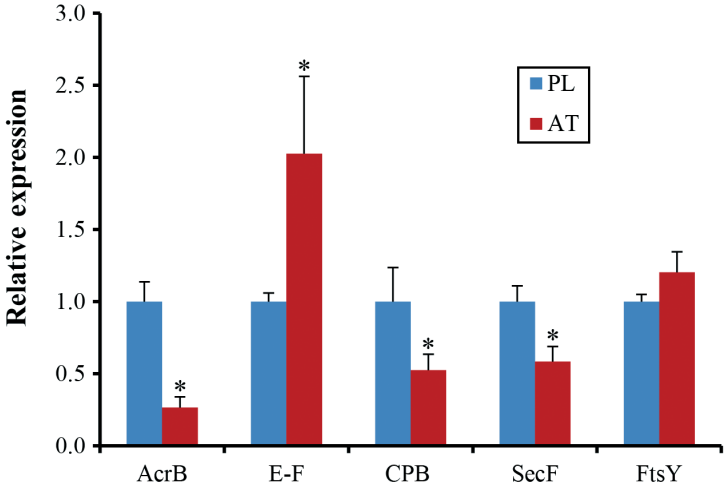

Fig. 5. Expression patterns of mRNA encoding 5 differentially expressed proteins (DEPs) in attached (AT) and planktonic (PL) cells. Samples for qRT-PCR were run in 3 biological replicates with 3 technical replicates. Error bars show standard deviation. ∗: significant difference between AT and PL cells ($p < 0.05$, 1-way ANOVA). AcrB: multidrug transporter AcrB; E-F: elongation factor P; CPB: capsular polysaccharide biosynthesis protein; SecF: protein-export membrane protein SecF; FtsY: signal recognition particle receptor FtsY

Resch et al. (2006) on comparative proteomic analysis of *Staphylococcus aureus* biofilms and planktonic cells, enzymes involved in pyruvate metabolism were up-regulated in biofilm cells. The involvement of pyruvate in biofilm formation was also suggested by Yeom et al. (2013), who used nuclear magnetic resonance (NMR)-based metabolite profiling of planktonic and biofilm cells of *Acinetobacter baumannii* 1656-2 and showed that the level of pyruvate, related to energy metabolism, was higher in the biofilm cells. Combined with our findings, it is reasonable to speculate that pyruvate metabolism plays an important and general role not only in the planktonic to sessile transition of bacteria but also in subsequent biofilm formation. The proteins involved in pyruvate metabolism of marine fouling bacteria may also be potential targets for future marine biofouling control applications.

We also found that the expression of a membrane OmpA-like protein was highly up-regulated in initially adherent cells of strain W-7 (AT/PL = 5.1). OmpA is an important outer membrane protein of gram-negative bacteria; it has been reported to have multiple functions, such as adhesion, invasion, and immune evasion, and to participate in biofilm formation (Smith et al. 2007, Namba et al. 2008). Namba et al. (2008) suggested that an OmpA homologue plays a role in the adhesion of *Aeromonas veronii* onto the intestinal surface of carp. Furthermore, in the marine fouling bacterium *Pseudoalteromonas* sp. D41, Ritter et al. (2012) found that the expression of an OmpA homologue was significantly up-regulated when the bacterium was grown in biofilms compared to planktonic cultures, indicating its involvement in biofilm formation. This involvement of OmpA in biofilm formation was supported by the finding that a *Pseudomonas aeruginosa* mutant unable to produce the OmpA homologue yielded biofilms with a lower biovolume and altered architecture (Ritter et al. 2012). In agreement with these studies, our study confirms the importance of OmpA in initial adhesion of marine fouling bacteria.

Furthermore, UTP-glucose-1-phosphate uridylyltransferase, also called UDP-glucose pyrophosphorylase (galU), was significantly up-regulated in initially adherent cells of strain W-7 compared with planktonic cells (AT/PL = 2.8); this may be relevant to the production of extracellular polysaccharides. GalU is responsible for the synthesis of UDP-glucose from glucose 1-phosphate and UTP, and UDP-glucose is a substrate in the biosynthesis of capsular polysaccharides, which presumably are produced to a greater extent in attached cells (Nesper et al. 2001, Guo et al. 2010, Zou et al. 2013). Extracellular polysaccharides are important components of exopolymeric substances (EPS) in bacteria, and EPS play vital roles in the attachment and biofilm formation of bacteria (Flemming & Wingender 2010, Flemming et al. 2016, Antunes et al. 2019). Zou et al. (2013) found that a galU mutant of *Haemophilus parasuis* SC096 was unable to form biofilms. Our results are consistent with these studies and indicate that galU

appears to play a role in the attachment of aquatic bacteria such as *Pseudoalteromonas* in addition to medically important species.

The planktonic to sessile transition of marine fouling bacteria is the first step in the formation of biofilms on surfaces and as such is important for early biofouling in marine environments. The present study reveals the candidate proteins (Table 3) that may be involved in this transition from planktonic life to an attached state. In addition to the previously discussed proteins such as OmpA, other DEPs were also found to change significantly in expression between planktonic and sessile states, including signal recognition particle receptor FtsY (reported to be associated with bacterial membrane protein biogenesis; Parlitz et al. 2007), phage-shock protein (reported to be associated with bacterial stress response; Darwin 2007), and elongation factor P (reported to mediate the synthesis of proteins required for bacterial growth, motility, virulence, and stress response; Doerfel & Rodnina 2013). This change in expression is indicative of the potential function of these proteins in bacterial attachment. Future investigations of the function of these candidate proteins in bacterial attachment pathways would deepen our understanding of the initial formation of biofilms and might provide molecular targets for developing methods to control early biofouling. Furthermore, it would be interesting in future work to compare protein expression in cells at the early stage of transitioning to a sessile lifestyle and those in established biofilms of *Pseudoalteromonas* sp. W-7; this could provide further information about which proteins specifically are involved during the planktonic to sessile transition.

In summary, 51 strains of marine bacteria were isolated from natural biofilms on artificial surfaces, among which a *Pseudoalteromonas* strain exhibited relatively strong biofilm-forming capacity and rapid attachment. The iTRAQ-based comparative proteomic analysis of planktonic and initially adhered cells of this strain (W-7) identified 163 DEPs that were mostly involved in cellular processes, metabolic processes, localization, cell part, membrane part, membrane, binding, catalytic activity, and transporter activity. Pyruvate metabolism, carbon fixation, and carbon metabolism may have significant roles in the attachment of *Pseudoalteromonas* sp. W-7. This study has furthered our understanding of the molecular mechanisms involved in the lifestyle transition of marine fouling bacteria from a planktonic to an adherent state. Future studies should investigate the roles of these DEPs in the planktonic to sessile transition of this bacterium.

Acknowledgements. This research was supported by the Chinese Ministry of Science and Technology through the National Key Research and Development Program of China under Grant 2018YFC1407505; the Youth Innovation Fund Project of Xiamen under Grant 3502Z20206053; the Science and Technology Project of Fujian Province under Grant 2018Y0076; the Project of Subsidy Funds for Marine Economic Development in Fujian Province under Grant FJHJF-L-2018-2; and the Key Laboratory of Marine Ecological Monitoring and Restoration Technology, Ministry of Nature Resources under Grant 2020ZX01. We thank Miaoqin Huang for help evaluating biofilm-forming capacity of marine bacteria.

LITERATURE CITED

Abioye OP, Loto CA, Fayomi OSI (2019) Evaluation of anti-biofouling progresses in marine application. J Bio Tribo Corros 5:22

Antunes J, Leão P, Vasconcelos V (2019) Marine biofilms: diversity of communities and of chemical cues. Environ Microbiol Rep 11:287–305

Arias-Barrau E, Olivera ER, Sandoval Á, Naharro G, Luengo JM (2006) Acetyl-CoA synthetase from *Pseudomonas putida* U is the only acyl-CoA activating enzyme induced by acetate in this bacterium. FEMS Microbiol Lett 260: 36–46

Bacchetti De Gregoris T, Khandeparker L, Anil AC, Mesbahi E, Burgess JG, Clare AS (2012) Characterisation of the bacteria associated with barnacle, *Balanus amphitrite*, shell and their role in gregarious settlement of cypris larvae. J Exp Mar Biol Ecol 413:7–12

Belas R (2013) When the swimming gets tough, the tough form a biofilm. Mol Microbiol 90:1–5

Belas R (2014) Biofilms, flagella, and mechanosensing of surfaces by bacteria. Trends Microbiol 22:517–527

Bowman JP (2007) Bioactive compound synthetic capacity and ecological significance of marine bacterial genus *Pseudoalteromonas.* Mar Drugs 5:220–241

Callow ME, Callow JA (2002) Marine biofouling: a sticky problem. Biologist (London) 49:10–14

Chandramouli KH, Dash S, Zhang Y, Ravasi T, Qian PY (2013) Proteomic and metabolomic profiles of marine *Vibrio* sp. 010 in response to an antifoulant challenge. Biofouling 29:789–802

Costerton JW, Cheng KJ, Geesey GG, Ladd TI, Nickel JC, Dasgupta M, Marrie TJ (1987) Bacterial biofilms in nature and disease. Annu Rev Microbiol 41:435–464

Darwin AJ (2007) Regulation of the phage-shock-protein stress response in *Yersinia enterocolitica*. In: Perry RD, Fetherston JD (eds) The genus *Yersinia*. Springer, New York, NY, p 167–177

Dobretsov S (2010) Marine biofilms. In: Dürr S, Thomason JC (eds) Biofouling. Blackwell, Oxford, p 123–136

Doerfel LK, Rodnina MV (2013) Elongation factor P: function and effects on bacterial fitness. Biopolymers 99:837–845

Dwivedi RC, Spicer V, Harder M, Antonovici M and others (2008) Practical implementation of 2D HPLC scheme with accurate peptide retention prediction in both dimensions for high-throughput bottom-up proteomics. Anal Chem 80:7036–7042

Egan S, James S, Holmström C, Kjelleberg S (2002) Correlation between pigmentation and antifouling compounds produced by *Pseudoalteromonas tunicata.* Environ Microbiol 4:433–442

Elifantz H, Horn G, Ayon M, Cohen Y, Minz D (2013) *Rhodobacteraceae* are the key members of the microbial community of the initial biofilm formed in Eastern Mediterranean coastal seawater. FEMS Microbiol Ecol 85: 348–357

Favre L, Ortalo-Magné A, Pichereaux C, Gargaros A, Burlet-Schiltz O, Cotelle V, Culioli G (2018) Metabolome and proteome changes between biofilm and planktonic phenotypes of the marine bacterium *Pseudoalteromonas lipolytica* TC8. Biofouling 34:132–148

Flemming HC, Wingender J (2010) The biofilm matrix. Nat Rev Microbiol 8:623–633

Flemming HC, Wingender J, Szewzyk U, Steinberg P, Rice SA, Kjelleberg S (2016) Biofilms: an emergent form of bacterial life. Nat Rev Microbiol 14:563–575

Gaddy JA, Tomaras AP, Actis LA (2009) The *Acinetobacter baumannii* 19606 OmpA protein plays a role in biofilm formation on abiotic surfaces and in the interaction of this pathogen with eukaryotic cells. Infect Immun 77: 3150–3160

Gilar M, Olivova P, Daly AE, Gebler JC (2005) Two-dimensional separation of peptides using RP-RP-HPLC system with different pH in first and second separation dimensions. J Sep Sci 28:1694–1703

Guo Y, Sagaram US, Kim J, Wang N (2010) Requirement of the *galU* gene for polysaccharide production by and pathogenicity and growth *in planta* of *Xanthomonas citri* subsp. *citri*. Appl Environ Microbiol 76:2234–2242

Hoke DE, Zhang K, Egan S, Hatfaludi T, Buckle AM, Adler B (2011) Membrane proteins of *Pseudoalteromonas tunicata* during the transition from planktonic to extracellular matrix-adherent state. Environ Microbiol Rep 3: 405–413

Holmström C, James S, Neilan BA, White DC, Kjelleberg S (1998) *Pseudoalteromonas tunicata* sp. nov., a bacterium that produces antifouling agents. Int J Syst Bacteriol 48: 1205–1212

Holmström C, Egan S, Franks A, McCloy S, Kjelleberg S (2002) Antifouling activities expressed by marine surface associated *Pseudoalteromonas* species. FEMS Microbiol Ecol 41:47–58

Huang YL, Dobretsov S, Xiong H, Qian PY (2007) Effect of biofilm formation by *Pseudoalteromonas spongiae* on induction of larval settlement of the polychaete *Hydroides elegans*. Appl Environ Microbiol 73:6284–6288

Huang YL, Ki JS, Case RJ, Qian PY (2008) Diversity and acyl-homoserine lactone production among subtidal biofilm-forming bacteria. Aquat Microb Ecol 52:185–193

Huggett MJ, Williamson JE, Nys RD, Kjelleberg S, Steinberg PD (2006) Larval settlement of the common Australian sea urchin *Heliocidaris erythrogramma* in response to bacteria from the surface of coralline algae. Oecologia 149:604–619

Hunsucker KZ, Vora GJ, Hunsucker JT, Gardner H and others (2018) Biofilm community structure and the associated drag penalties of a groomed fouling release ship hull coating. Biofouling 34:162–172

Lane DJ (1991) 16S/23S rRNA sequencing. In: Stackebrandt E, Goodfellow M (eds) Nucleic acid techniques in bacterial systematics. Wiley, Chichester, p 115–175

Leary DH, Li RW, Hamdan LJ, Hervey WJ IV and others (2014) Integrated metagenomic and metaproteomic analyses of marine biofilm communities. Biofouling 30: 1211–1223

Leo JC, Skurnik M (2011) Adhesins of human pathogens from the genus *Yersinia*. In: Linke D, Goldman A (eds) Bacterial adhesion. Springer, Dordrecht, p 1–15

Leroy C, Delbarre-Ladrat C, Ghillebaert F, Rochet MJ, Compère C, Combes D (2007) A marine bacterial adhesion microplate test using the DAPI fluorescent dye: a new method to screen antifouling agents. Lett Appl Microbiol 44:372–378

Li YF, Guo XP, Yang JL, Liang X and others (2014) Effects of bacterial biofilms on settlement of plantigrades of the mussel *Mytilus coruscus*. Aquaculture 433:434–441

Liang X, Peng LH, Zhang S, Zhou S and others (2019) Polyurethane, epoxy resin and polydimethylsiloxane altered biofilm formation and mussel settlement. Chemosphere 218:599–608

Lin PY, Chen HL, Huang CT, Su LH, Chiu CH (2010) Biofilm production, use of intravascular indwelling catheters and inappropriate antimicrobial therapy as predictors of fatality in *Chryseobacterium meningosepticum* bacteraemia. Int J Antimicrob Agents 36:436–440

Mack D (1999) Molecular mechanisms of *Staphylococcus epidermidis* biofilm formation. J Hosp Infect 43(Supplement):S113–S125

Mosier AC, Li Z, Thomas BC, Hettich RL, Pan C, Banfield JF (2015) Elevated temperature alters proteomic responses of individual organisms within a biofilm community. ISME J 9:180–194

Namba A, Mano N, Takano H, Beppu T, Ueda K, Hirose H (2008) OmpA is an adhesion factor of *Aeromonas veronii*, an optimistic pathogen that habituates in carp intestinal tract. J Appl Microbiol 105:1441–1451

Nesper J, Lauriano CM, Klose KE, Kapfhammer D, Kraiß A, Reidl J (2001) Characterization of *Vibrio cholerae* O1 El Tor *galU* and *galE* mutants: influence on lipopolysaccharide structure, colonization, and biofilm formation. Infect Immun 69:435–445

Parlitz R, Eitan A, Stjepanovic G, Bahari L, Bange G, Bibi E, Sinning I (2007) *Escherichia coli* signal recognition particle receptor FtsY contains an essential and autonomous membrane-binding amphipathic helix. J Biol Chem 282: 32176–32184

Peeters E, Nelis HJ, Coenye T (2008) Comparison of multiple methods for quantification of microbial biofilms grown in microtiter plates. J Microbiol Methods 72:157–165

Rao D, Webb JS, Kjelleberg S (2005) Competitive interactions in mixed-species biofilms containing the marine bacterium *Pseudoalteromonas tunicata*. Appl Environ Microbiol 71:1729–1736

Resch A, Leicht S, Saric M, Pásztor L, Jakob A, Götz F, Nordheim A (2006) Comparative proteome analysis of *Staphylococcus aureus* biofilm and planktonic cells and correlation with transcriptome profiling. Proteomics 6:1867–1877

Ritter A, Com E, Bazire A, Goncalves MDS and others (2012) Proteomic studies highlight outer-membrane proteins related to biofilm development in the marine bacterium *Pseudoalteromonas* sp. D41. Proteomics 12:3180–3192

Romero M, Avendaño-Herrera R, Magariños B, Cámara M, Otero A (2010) Acylhomoserine lactone production and degradation by the fish pathogen *Tenacibaculum maritimum*, a member of the *Cytophaga-Flavobacterium-Bacteroides* (CFB) group. FEMS Microbiol Lett 304: 131–139

Saravanan P, Nancharaiah YV, Venugopalan VP, Rao TS, Jayachandran S (2006) Biofilm formation by *Pseudoalteromonas ruthenica* and its removal by chlorine. Biofouling 22:371–381

Shikuma NJ, Pilhofer M, Weiss GL, Hadfield MG, Jensen GJ, Newman DK (2014) Marine tubeworm metamorphosis induced by arrays of bacterial phage tail-like structures. Science 343:529–533

Smith SGJ, Mahon V, Lambert MA, Fagan RP (2007) A molecular Swiss army knife: OmpA structure, function and expression. FEMS Microbiol Lett 273:1–11

Vandecandelaere I, Segaert E, Mollica A, Faimali M, Vandamme P (2008) *Leisingera aquimarina* sp. nov., isolated from a marine electroactive biofilm, and emended descriptions of *Leisingera methylohalidivorans* Schaefer et al. 2002, *Phaeobacter daeponensis* Yoon et al. 2007 and *Phaeobacter inhibens* Martens et al. 2006. Int J Syst Evol Microbiol 58:2788–2793

Wang X, Li Z, Su J, Tian Y, Ning X, Hong H, Zheng T (2010) Lysis of a red-tide causing alga, *Alexandrium tamarense*, caused by bacteria from its phycosphere. Biol Control 52: 123–130

Wang X, Huang Y, Sheng Y, Su P, Qiu Y, Ke C, Feng D (2017) Antifouling activity towards mussel by small-molecule compounds from a strain of *Vibrio alginolyticus* bacterium associated with sea anemone *Haliplanella* sp. J Microbiol Biotechnol 27:460–470

Xie Q, Pan J, Ma C, Zhang G (2019) Dynamic surface antifouling: mechanism and systems. Soft Matter 15:1087–1107

Xu D, Xia J, Zhou E, Zhang D and others (2017) Accelerated corrosion of 2205 duplex stainless steel caused by marine aerobic *Pseudomonas aeruginosa* biofilm. Bioelectrochemistry 113:1–8

Yang F, Shen Y, Camp DG II, Smith RD (2012) High-pH reversed-phase chromatography with fraction concatenation for 2D proteomic analysis. Expert Rev Proteomics 9:129–134

Yang JL, Shen PJ, Liang X, Li YF, Bao WY, Li JL (2013) Larval settlement and metamorphosis of the mussel *Mytilus coruscus* in response to monospecific bacterial biofilms. Biofouling 29:247–259

Yang JL, Li YF, Guo XP, Liang X and others (2016a) The effect of carbon nanotubes and titanium dioxide incorporated in PDMS on biofilm community composition and subsequent mussel plantigrade settlement. Biofouling 32:763–777

Yang JL, Li YF, Liang X, Guo XP and others (2016b) Silver nanoparticles impact biofilm communities and mussel settlement. Sci Rep 6:37406

Yebra DM, Kiil S, Dam-Johansen K (2004) Antifouling technology — past, present and future steps towards efficient and environmentally friendly antifouling coatings. Prog Org Coat 50:75–104

Yeom J, Shin JH, Yang JY, Kim J, Hwang GS (2013) ^{1}H NMR-based metabolite profiling of planktonic and biofilm cells in *Acinetobacter baumannii* 1656-2. PLOS ONE 8:e57730

Yildiz FH, Visick KL (2009) *Vibrio* biofilms: so much the same yet so different. Trends Microbiol 17:109–118

Zeng Z, Guo XP, Li B, Wang P and others (2015) Characterization of self-generated variants in *Pseudoalteromonas lipolytica* biofilm with increased antifouling activities. Appl Microbiol Biotechnol 99:10127–10139

Zeng Z, Guo XP, Cai X, Wang P, Li B, Yang JL, Wang X (2017) Pyomelanin from *Pseudoalteromonas lipolytica* reduces biofouling. Microb Biotechnol 10:1718–1731

Zou Y, Feng S, Xu C, Zhang B and others (2013) The role of *galU* and *galE* of *Haemophilus parasuis* SC096 in serum resistance and biofilm formation. Vet Microbiol 162: 278–284

Editorial responsibility: Staffan Kjelleberg, Sydney, New South Wales, Australia
Reviewed by: 3 anonymous referees

Submitted: July 23, 2020
Accepted: December 28, 2020
Proofs received from author(s): March 27, 2021